J. Physiol. (1985), **367**, *pp.* 117–141
With 12 text-figures
Printed in Great Britain

POTASSIUM CHANNELS IN CULTURED BOVINE ADRENAL CHROMAFFIN CELLS

BY ALAIN MARTY* AND ERWIN NEHER†

*From the *Laboratoire de Neurobiologie, Ecole Normale Supérieure, 46, Rue D'Ulm, F-75005 Paris, France, and the †Max-Planck-Institut für biophysikalische Chemie Am Faßberg, D-3400 Göttingen, F.R.G.*

(*Received 7 February 1985*)

SUMMARY

1. K channels of bovine adrenal chromaffin cells were studied using patch-clamp techniques.

2. Whole-cell K currents measured near +10 mV were much larger in 1 mM-external Ca than in Ca-free saline. Noise analysis suggested that this Ca-dependent current was carried by a large unitary conductance channel, called BK channel, which was previously described in inside-out patches (Marty, 1981).

3. The Ca-dependent K current near +10 mV declined with time due to 'run-down' of Ca channels. At the same time, a fraction of the outward current observed above +50 mV was also eliminated. This outward current component probably represents K efflux through Ca channels.

4. Whole-cell Ca-dependent K currents were studied using various Ca buffers. EGTA buffers were surprisingly inefficient: in order to block the current entirely, it was necessary to use an isotonic EGTA solution and to increase internal pH. 1,2-bis(*o*-aminophenoxy)ethane-*N*,*N*,*N*′,*N*′-tetraacetic acid (BAPTA) was at least five times more efficient than EGTA.

5. In isolated patches three types of single-channel K currents were observed. Under normal ionic conditions (140 mM-K inside, 140 mM-Na outside), the unitary conductances measured between −20 and +40 mV were 96 pS, 18 pS and 8 pS. The 96 pS channels are the Ca-dependent BK channels.

6. 18 pS and 8 pS channels were both activated and then inactivated by membrane depolarization. Both displayed complex kinetics; single-channel currents were grouped in bursts. Activation and inactivation kinetics were faster for the 18 pS channel (therefore termed FK channel, for fast K channel) than for the 8 pS channel (SK channel, for slow or small amplitude channel). The voltage dependence of opening probability was steeper for the FK channel as compared to the SK channel.

INTRODUCTION

The study of voltage-dependent K currents in nerve axons and in the cell bodies of neurones has led to the demonstration of a variety of channel types. In neuronal cell bodies, several components can be distinguished on the basis of activation and inactivation kinetics, voltage dependence and sensitivity to extracellular blocking

agents (reviewed in Thompson & Aldrich, 1980; Hermann & Hartung, 1983). One of these currents depends on the presence of extracellular Ca (Meech & Standen, 1975; Heyer & Lux, 1976). Nerve axons have been thought to possess a more homogeneous class of K currents, but recently, closer analysis also revealed a variety of channel types (reviewed by Dubois, 1983).

Chromaffin cells of the adrenal medulla fire action potentials at rest, and the spike frequency is enhanced by acetylcholine (Biales, Dichter & Tischler, 1976; Brandt, Hagiwara, Kidokoro & Miyazaki, 1976). The action potentials result from voltage-dependent Na, Ca and K currents similar to those of neurones and muscle fibres (Biales *et al.* 1976; Brandt *et al.* 1976; Kidokoro & Ritchie, 1980).

In a previous investigation (Fenwick, Marty & Neher, 1982*a*, *b*), we studied chromaffin cell Na and Ca currents both at a macroscopic (cellular) level and as single-channel events. The present paper aims at establishing a first classification of K channels in chromaffin cells, and to relate cell-current components to their single-channel counterparts. One type of K channel, a Ca-dependent K channel of big unitary amplitude (termed BK channel), has already been characterized (Marty, 1981). In the course of the work, it appeared that Ca-dependent K channels may be activated by Ca influx in cells which are dialysed with a comparatively large concentration of the Ca-buffer EGTA. This observation led us to examine how the Ca-buffering capacity of the internal solution affects Ca-dependent K currents.

METHODS

Preparation and recording

The methods used to obtain cells and to perform recordings were similar to those described before (Fenwick *et al.* 1982*a*). We only summarize here alterations with respect to previous procedures. The medullas from two to three adrenal glands were sliced, and cut into small pieces. They were washed with Locke solution and subsequently incubated in 25 ml of Locke solution supplemented with Worthington (CLS II) collagenase 0·5 mg/ml for 30 min under 5 % CO_2, 95 % O_2 in a shaking water-bath at 35 °C. This was followed by two similar incubation periods in 10 mg/15 ml of Sigma Type IV collagenase. During these incubations the tissue was repeatedly triturated by sucking through plastic pipettes, the openings of which had been widened to 3–5 mm. Supernatants from the latter two incubation periods were collected and stored on ice. The remaining tissue was again triturated and filtered through 80 μm diameter nylon mesh, rinsing with Locke solution. The collected cell suspensions were washed by centrifugation (300 *g* for 6 min) and purified by Percoll gradient centrifugation as described previously (Fenwick *et al.* 1982*a*). The cells were maintained in tissue culture (Medium 199, supplemented by 10 % fetal calf serum, 1 mg bovine serum albumin/ml and antibiotics) for 1–8 days before use. Cell currents were studied using the four recording configurations described by Hamill, Marty, Neher, Sakmann & Sigworth, 1981 ('cell-attached', 'whole-cell', 'inside-out' and 'outside-out' modes).

In most experiments, the membrane potential was held at −80 mV. (If the pipette and bath solutions were different, appropriate corrections were applied to the command potential so that the effective membrane holding potential was in all cases −80 mV.) 60 ms or 100 ms long depolarizing voltage pulses were given with a frequency of 0·5–0·7 Hz. Alternatively a two-pulse protocol was used as described later. The resting cell resistance, measured in whole-cell recordings between −150 and −60 mV, was typically in the range of 10 GΩ. The corresponding leakage current was less than 40 pA at the largest voltage steps (180 mV), whereas cell K currents were usually of several nanoamperes. Correction of I–V curves for leakage conductance was therefore usually unnecessary. Whole-cell records were filtered at 2·5 kHz (−3dB) unless stated otherwise.

Single-channel currents were recorded on tape and later replayed, filtered at 1·6 kHz and digitized at 0·2 ms interval for analysis. Single-channel amplitudes were determined either with the support

of an interactive computer program (see Sigworth, 1983*a*) or else measured directly from chart paper or the storage oscilloscope screen. Recordings of the responses to individual stimulus episodes were corrected for leakage and capacitance artifacts by subtracting the averaged and scaled version of a response to a hyperpolarizing stimulus of one half amplitude. The correction of large capacitance artifacts was not always complete due to saturation of the tape recorder.

Series-resistance compensation

The efficiency of the whole-cell voltage clamp depends on the access resistance of the pipette tip, R_s. In the present work wide-tipped pipettes were used, with resistances of 1·5–2 MΩ as measured in normal saline. Once in the whole-cell recording mode the value of R_s was found to be substantially higher. This value was checked regularly during each experiment, and suction was applied to the pipette interior, in order to re-establish a current pathway, whenever R_s increased above 10 MΩ. In most recordings the R_s value remained between 2 and 5 MΩ. Analog compensation of R_s was applied using the method of Sigworth (1983*b*). This allowed us to bring the effective R_s value, R_e, down to between 1 and 1·5 MΩ. Cells had an input capacitance of 5–10 pF, so that voltage-clamp time constants ranged between 5 and 15 μs. Since maximal values of outward currents were less than 5 nA, the voltage drop across the series resistance introduced an error of less than 7·5 mV. This residual error was taken into account in $I-V$ plots of plateau current and in potential values indicated in Figures.

A low R_e value turned out to be essential in the study of Ca-dependent K currents. A typical artifact which could be observed on cells with high R_e values, or in the absence of series resistance compensation, was a greatly reduced rate of rise of the current for clamp potentials between +20 and +50 mV. In this potential range the Ca-dependent current diminishes with potential (see Results below) and the slope conductance is typically −0·05 to −0·2 μS, corresponding to a negative resistance of 5–20 MΩ. If R_e were comparable or larger than this resistance, then the membrane potential would not be effectively clamped and it would shift to less positive values until a region of the $I-V$ curve with a slope less than $1/R_e$ would be reached. This explains the anomalous rising phase seen with large R_e values in this potential range.

Solutions

The standard extracellular solution contained, in mM: 140, NaCl; 2, $MgCl_2$; 1, $CaCl_2$; 2·8, KCl; 10, HEPES–NaOH; pH, 7·2. The internal solution contained 2 mM-$MgCl_2$, 10 mM-HEPES–KOH, a Ca buffer and KCl. The pH was adjusted with KOH either to 7·2 or to 8·2. KCl was added at a concentration such that the total internal K concentration was 150 mM. In many experiments the Na current was blocked by addition of tetrodotoxin (TTX, 7–15 μM) to the external solution. To study the effects of external Ca on K current, an external solution was used which contained 0·5 mM-EGTA and no Ca. The Ca-free solution was applied with a fast microperfusion system, which had an exchange time of about 100 ms (Fenwick *et al.* 1982*a*).

For Ca buffering of the intracellular solution we used either EGTA or 1,2-bis(*o*-aminophenoxy)ethane-*N*,*N*,*N*′,*N*′-tetraacetic acid (BAPTA). Both buffers have an apparent association constant close to 10^7 M^{-1} (Tsien, 1980) and are highly selective for Ca against Mg. Thus, the equilibrium buffering capacities defined as $d[Ca_t]/d[Ca]$, where $[Ca_t]$ and [Ca] are the total concentration of Ca and the free concentration of Ca respectively, are approximately the same. Nevertheless, we observed large differences in the buffering capacity of the two substances. The differences probably can be explained by kinetic considerations, since, as pointed out by Tsien (1980), BAPTA has much higher apparent association and dissociation rates than EGTA at pH 7·2. In this context it should be mentioned that the buffering power of BAPTA is almost independent of hydrogen ion concentration at pH 7 and above. Buffering by EGTA, on the other hand, is very dependent on pH since EGTA is doubly protonated at neutral pH.

Table 1 gives the buffers used, together with values for equilibrium buffer capacity as defined above and the free-Mg concentration expected. The latter values were calculated from Martell & Smith's (1974) stability constants for EGTA (20 °C, 0·1 M ionic strength); values for BAPTA were taken from Tsien (1980).

All experiments were performed at room temperature (22–28 °C).

Noise analysis

Ensemble fluctuation analysis (Sigworth, 1980) was carried out on outward current responses to voltage steps. Usually four groups of eight individual sweeps were used. In each group, the mean current was determined, and the variance around this mean was estimated. Then over-all means of current and variance were obtained over the four groups. The main sources of error encountered were due to inactivation of Ca-independent K channels and decrease in Ca-dependent currents as a result of wash-out of Ca channels. To minimize the first source of drift, analysis of Ca-independent currents started at least five sweeps after the onset of a series of pulses. This assured that a steady response was reached. Analysis of Ca-dependent currents was restricted to the first minutes of whole-cell recording, when run-down was still very slow. With these precautions, the relative amplitude changes between consecutive sweeps were less than 3×10^{-3}, and the error on the variance was calculated to be less than 3%.

TABLE 1. Ca buffers, added to the intracellular solution

Buffer (mM)	[Mg] (mM)	Equilibrium Ca buffering capacity
0·5 EGTA pH 7·2	2·0	$4·8 \times 10^3$
11 EGTA/1 Ca pH 7·2	1·2	$8·2 \times 10^4$
64 EGTA/6 Ca pH 7·2	0·5	$6·0 \times 10^5$
11 EGTA/1 Ca pH 8·2	0·12	$6·1 \times 10^6$
64 EGTA/6 Ca pH 8·2	0·02	$4·2 \times 10^7$
1·1 BAPTA/0·1 Ca pH 7·2	1·9	$7·0 \times 10^3$
5·5 BAPTA/0·5 Ca pH 7·2	1·6	$3·6 \times 10^4$

All these buffers maintain pCa at 8 or higher.

Equilibrium buffer capacity was calculated as $d[Ca_t]/d[Ca]$, where $[Ca_t]$ is the total concentration of Ca and [Ca] the concentration of free Ca.

RESULTS

Ca-dependent K currents in whole-cell recordings

In a cell dialysed with the standard intracellular solution and bathed in saline containing TTX, voltage steps elicited outward currents as illustrated in Fig. 1. The underlying conductance was K selective, since (1) the currents, which were outward in the presence of 140 mM-Na in the external solution, reversed at 0 mV upon replacing Na with K in the bath, and (2) the currents were not observed in Cs-dialysed cells. K currents started to turn on for test potentials of −40 mV or above. Between −40 and −20 mV, the currents activated slowly after some delay (Fig. 1). Between −20 and +40 mV, the K currents varied greatly depending on whether Ca was present in the external solution (Fig. 1*A*) or not (Fig. 1*B*). Between +50 and +100 mV, on the other hand, the currents were similar (but not identical) with and without external Ca ions. When the Ca-free solution was applied rapidly with the fast microperfusion system (see Methods), its effects on K currents were fast (in the range of the exchange time of the system, i.e. 100 ms), stable and reversible.

Fig. 1*C* represents the *I–V* curves corresponding to the plateau currents of Fig. 1*A* and *B*. The two curves cross over at +52 mV. Below this potential, the curve in 1 mM-Ca lies above the curve in 0 mM-Ca, with a peak Ca-dependent current near +10 mV. Above the cross-over potential, currents are found to be smaller in 1 mM-Ca than in 0 mM-Ca.

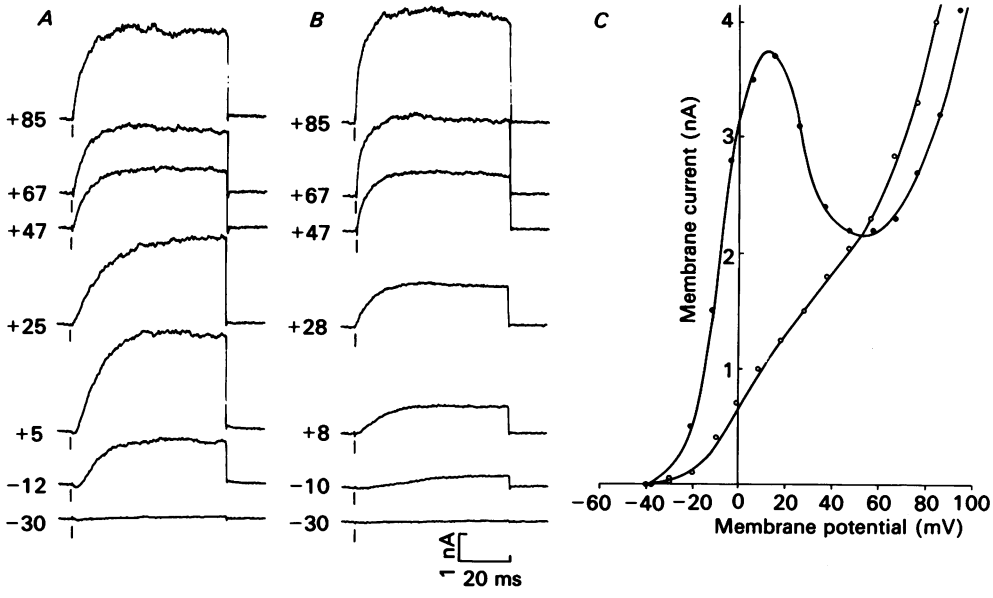

Fig. 1. Influence of external Ca ions on outward currents. Responses to positive voltage steps to different test potentials, obtained in normal saline (*A*), or after replacement of Ca (normal concentration 1 mM) with 0·5 mM-EGTA (*B*). Cell capacitance 7·3 pF. Access resistance $R_s = 3$ MΩ; effective access resistance after compensation (see Methods) $R_e = 1{\cdot}2$ MΩ. Holding potential −80 mV (as in all subsequent Figures). Traces are corrected for leakage and capacitive current. The numbers next to each trace indicate the potential (in mV) which is reached at the plateau current level, taking into account the voltage drop across R_e. The onsets of the voltage pulses are marked by vertical bars below or above individual traces in all Figures. Na currents were blocked with tetrodotoxin (10 μg/ml). *C*, *I–V* relationships of the plateau currents in the presence (filled symbols) and in the absence (open symbols) of external Ca. The two curves cross over at +52 mV.

Meech & Standen (1975), who observed a Ca-dependent 'hump' similar to that of Fig. 1 in *I–V* curves obtained in snail neurones, proposed that Ca was acting on K channels from the intracellular side of the membrane, where its concentration was raised following Ca entry through voltage-dependent Ca channels. Under the ionic conditions of Fig. 1, currents through Ca channels in chromaffin cells have an activation threshold near −20 mV, a peak near +10 mV, and a reversal potential of +50 mV (Fenwick *et al.* 1982*b*). This is in excellent agreement with the characteristics of the Ca-dependent K current of Fig. 1. However, the agreement may be to some extent fortuitous as far as the cross-over potential is concerned. First, even at the reversal potential for Ca channels, there may be a small influx of Ca (compensated by an efflux of monovalent cations) which could activate K channels to some extent.

Secondly, the previous measurements were obtained in Cs-dialysed cells, whereas the pipette solution contained K in the experiment of Fig. 1. As will be discussed below, Ca currents are probably similar in K-, Na- or Cs-dialysed cells. The reversal potential value may nevertheless differ slightly for K- and Cs-containing cells, as has been shown previously in heart muscle cells (Lee & Tsien, 1982).

Above +50 mV, the outward current was smaller in 1 mM-Ca than in the Ca-free solution. This effect was consistently observed in all experiments, regardless of whether the Ca-free solution contained 0·5 mM-EGTA, as in the example of Fig. 1, or 1 mM-Co, as was the case in some experiments. It seemed very unlikely that significant transfer of Ca ions through the membrane would occur above the reversal potential. Thus, the augmentation of K current in Ca-free solution above +50 mV was probably not linked to change of intracellular Ca concentration. On the other hand, it was tempting to relate this extra current to the outflow of K through Ca channels. The fact that monovalent cations can carry outward current through Ca channels at large positive potentials has been demonstrated in chromaffin cells (Fenwick *et al.* 1982*b*) and in heart muscle cells (Lee & Tsien, 1982). Furthermore, it is known that divalent ions such as Ca block influx of monovalent ions through the channels, in the voltage range comprised between −50 and +50 mV (Kostyuk & Krishtal, 1977; Kostyuk, Mironov & Shuba, 1983; Almers & McCleskey, 1984; Almers, McCleskey & Palade, 1984; Hess & Tsien, 1984). It is therefore plausible that external Ca ions blocked the outflux of monovalent ions (mostly K) above +50 mV in the experiment of Fig. 1*A*. The finding that replacement of Ca by Co also results in an augmented outward current above +50 mV implies then that Co is not as efficient as Ca in blocking the flow of monovalent ions (see also Almers, McCleskey & Palade, 1984).

Slow decline of Ca-dependent currents

Ca currents subside over a time course of about 20 min in our recording conditions (Fenwick *et al.* 1982*b*). It was therefore expected that the Ca-dependent hump of the plateau *I–V* curve would be gradually suppressed as the Ca entry decreased. This was in fact the case. The reduction of the Ca-dependent hump paralleled the run-down of Ca currents in two ways. First, it had a similar time course, with an initial plateau lasting several minutes, and a half-decline time of about 10 min (see Fenwick *et al.* 1982*b*). Secondly, the amplitude of Ca currents could be roughly evaluated in K-dialysed cells by estimating the early inward current obtained between −20 and +20 mV (Fig. 1, see trace at −12 mV). This early Ca current and the late Ca-dependent K current decreased simultaneously as the number of functional Ca channels in the membrane diminished.

It has been shown that the current carried by monovalent ions through Ca channels also subsides during run-down (Fenwick *et al.* 1982*b*). This effect was only observed at large positive potentials, because the external Ca ions present in normal saline blocked monovalent ion flow at lower potentials. Comparison of *I–V* curves obtained in Ca-free saline before and after run-down should in principle yield the full *I–V* curve of monovalent cation current through Ca channels. Fig. 2 shows the two *I–V* curves for the same cell as in Fig. 1. Fig. 2*A* illustrates current records obtained 16 min after the start of the whole-cell recording. At this stage, no inward current at all was

observed between −20 and +20 mV, and the traces were identical in 1 mM-Ca and in Ca-free saline. The currents remained as shown in Fig. 2*A* for tens of minutes without any noticeable change.

Fig. 2*B* shows the (identical) *I–V* plots in 1 mM-Ca and in Ca-free saline after

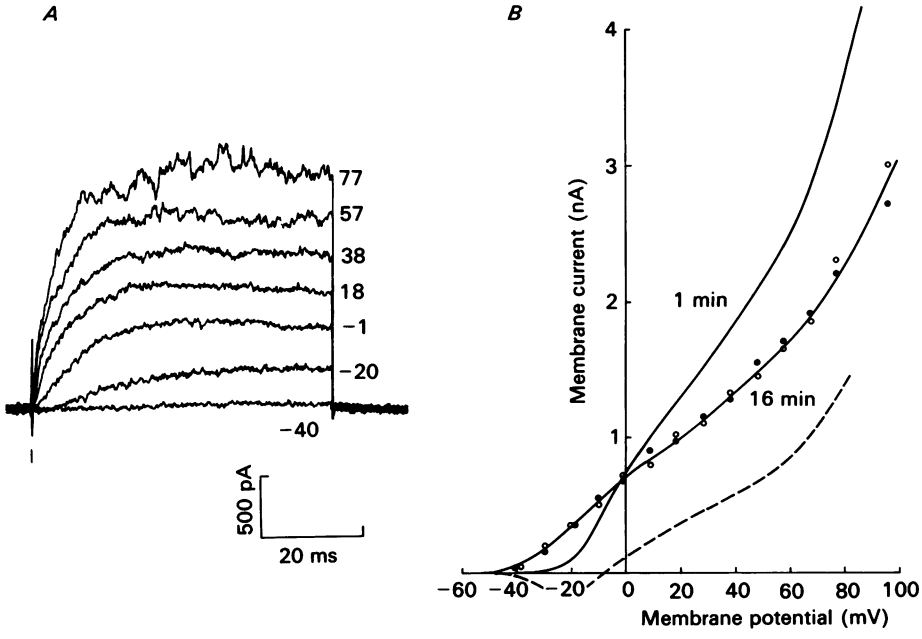

Fig. 2. Outward currents after run-down of Ca currents. *A*, responses to positive voltage steps of 40–160 mV amplitude, in 20 mV increments, obtained in the same cell as in Fig. 1 after complete run-down of Ca currents. Effective test potentials are indicated near the end of each trace. The records were taken 16 min after the start of whole-cell recording in normal saline. At this stage of the experiment, no inward current was seen between −20 and +20 mV at the beginning of voltage steps (compare the results with those of Fig. 1); furthermore, responses were totally unaffected by removal of external Ca. *B*, *I–V* curves in the presence (filled symbols) and in the absence (open symbols) of external Ca. The *I–V* curve of Fig. 1 in Ca-free saline, which was obtained 1 min after the start of the whole-cell recording, is shown for comparison. The dashed line represents the *I–V* curve for monovalent ion current flow through Ca channels. It was obtained by subtracting the curve at 16 min, shifted by 5 mV towards positive potentials, from the curve at 1 min.

run-down, and also shows the *I–V* curve of Fig. 1 in Ca-free saline for comparison. The current before run-down is smaller than that after run-down for potentials between −40 and 0 mV. Above 0 mV, the situation is reversed. The difference between the two curves indicates that the monovalent ion current is inward at negative potentials and outward at positive potentials. The exact value of the reversal potential is probably somewhat more negative than the cross-over point, because *I–V* curves are slowly shifted to the left during the course of whole-cell recording (Marty & Neher, 1983; Fernandez, Fox & Krasne, 1984). If a 5 mV shift is taken into account (a value taken from Marty & Neher, 1983; Fig. 7), the reversal potential is found to be −7 mV in the experiment shown (Fig. 2, dashed curve). This estimate of the

reversal potential of monovalent currents with K ions inside and Na ions outside indicates that the channels have similar permeabilities for the two cations. In their early study in snail neurones, Kostyuk & Krishtal (1977) found a reversal potential of +10 to +20 mV under similar ionic conditions.

Comparison of the continuous and dashed lines in Fig. 2 gives an estimate of the proportion of the total current which is due to monovalent ions crossing Ca channels under standard recording conditions. At +80 mV, this proportion is as high as 40% in the experiment shown, and similar results were found in other cells. Thus, in Ca-free solution, a very large fraction of the total current observed at positive potentials is due to Ca channels rather than to K channels.

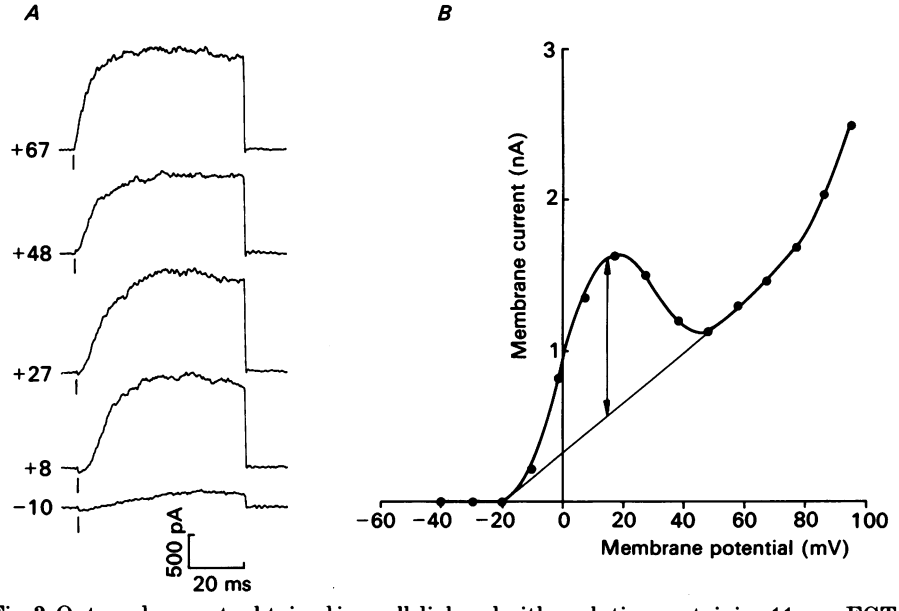

Fig. 3. Outward currents obtained in a cell dialysed with a solution containing 11 mM-EGTA and 1 mM-Ca at pH 8·2. *A*, responses to positive voltage steps of 70–150 mV amplitude, from a holding potential of −80 mV. Cell capacitance 4·5 pF. *B*, plateau *I–V* curve, showing the characteristic hump between 0 and +40 mV. The method of measurement of the Ca-dependent current is illustrated (arrows).

Ca-dependent currents as a function of intracellular Ca buffer

It was surprising that the chromaffin cells had Ca-dependent K currents of several nanoamperes even though they were dialysed with a Ca buffer made up with 1 mM-Ca and 11 mM-EGTA. An immediate question was whether the amplitude of the Ca-dependent K current would be affected by either reducing or increasing the buffering capacity of the internal solution. Internal solutions of seven different compositions were tested, with Ca-buffering capacities varying over a $1–2 \times 10^4$ range. In four solutions, the Ca-buffering capacity was modified by changing either the total EGTA concentration or the pH (see Methods for pH effects).

In one of the solutions tested, the equilibrium buffer capacity was increased by a factor of approximately 100 by raising pH to 8·2, while keeping the same EGTA and

Ca concentrations as in the reference buffer (11 and 1 mM, respectively). Under such circumstances, *I–V* curves in 1 mM-external Ca still displayed a hump in ten out of eleven cells tested. An example is shown in Fig. 3.

To further increase the Ca-buffering capacity, a solution containing 64 mM-EGTA and 6 mM-Ca at pH 8·2 was used. We chose 64 mM-EGTA–KOH because it gave the same K concentration as our standard intracellular saline (see Methods). With this

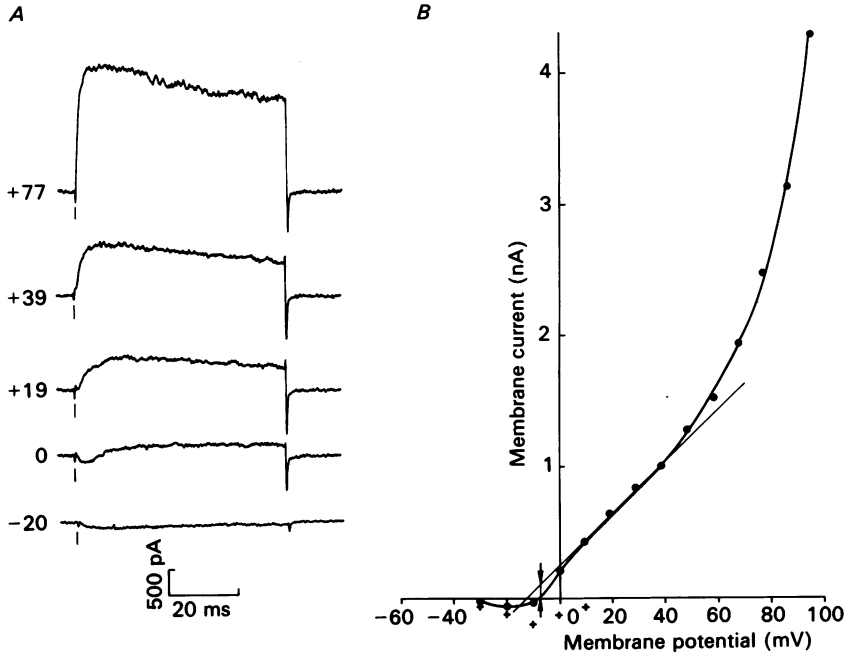

Fig. 4. Membrane currents in a cell dialysed with a solution containing 64 mM-EGTA/6 mM-Ca at pH 8·2. *A*, currents in response to voltage steps reaching the indicated test potentials. Leakage and capacitance currents have been subtracted. The bath solution contained 1 mM-Ca. Low-pass filter 1·2 kHz. Cell capacitance 7·2 pF. *B*, *I–V* curve from the results in *A*. Up to 0 mV the current was measured at the end of the 60 mV pulse. Above 0 mV, peak currents were plotted instead. Crosses: peak inward currents. The method for measuring Ca-dependent current gives a negative value (arrows) in this case.

solution, no indication of a hump could be detected in 1 mM-external Ca (Fig. 4). Due to the lack of Ca-activated K currents a clear inward Ca current was now visible between −20 and 0 mV (crosses in Fig. 4). At positive potentials, Ca currents were obscured by Ca-independent K currents.

To obtain an estimate of the peak Ca-dependent current, a graphic method was employed as shown in Figs. 3 and 4. When a 'hump' was present near +10 mV, a tangent to the *I–V* curve in the voltage range near −10 and +50 mV was drawn, and the maximal current above the tangent was measured (Fig. 3). When no hump was observed, the tangent at the inflexion point of the *I–V* curve (near +20 mV) was taken as reference (Fig. 4).

Average values obtained with the graphic method of Figs. 3 and 4 are given in

Table 2. A buffer containing only 0·5 mM-EGTA, with low equilibrium buffering capacity, gave currents only slightly larger than the reference 11 mM-EGTA/1 mM-Ca buffer. Similar results were obtained with a 1·1 mM-BAPTA/0·1 mM-Ca buffer, which has also a much weaker equilibrium buffering capacity than the reference solution. On the other hand, two other solutions containing 64 mM-EGTA/6 mM-Ca

TABLE 2. Ca currents and Ca-dependent K currents in various intracellular Ca buffers

Intracellular Ca buffer (mM)	Ca current (pA/pF)	Ca-dependent K current (pA/pF)
0·5 EGTA pH 7·2	17·5 ± 7·4 (3)	450 ± 220 (7)
11 EGTA/1 Ca pH 7·2	21 ± 13 (4)	240 ± 120 (8)
64 EGTA/6 Ca pH 7·2	—	30 ± 21 (3)
11 EGTA/1 Ca pH 8·2	29 ± 14 (4)	170 ± 110 (7)
64 EGTA/6 Ca pH 8·2	—	−10 ± 32 (6)
1·1 BAPTA/0·1 Ca pH 7·2	—	360 ± 150 (4)
5·5 BAPTA/0·5 Ca pH 7·2	—	40 ± 14 (5)

All measurements were obtained between 1 and 3 min after the start of whole-cell recording. The total cell currents have been divided by the cell capacitance (which was always comprised between 5 and 10 pF) to eliminate variations linked to cell size. Means, standard deviations and number of cells are given. The second column indicates peak Ca currents in Cs-dialysed cells. The third column shows Ca-dependent K currents in K-dialysed cells. To estimate this current, a graphic method was used as shown in Figs. 3 and 4.

and 5·5 mM-BAPTA/0·5 mM-Ca respectively at pH 7·2 gave very small Ca-dependent currents, only slightly larger than those of Fig. 4.

Comparison of the results of Table 2 with the calculations of Table 1 shows that the amplitude of Ca-dependent K currents does not follow the order of equilibrium buffering capacities. Two discrepancies may be noticed. First, the 64 mM-EGTA/6 mM-Ca, pH 7·2 solution has a weaker buffering power than the 11 mM-EGTA/1 mM-Ca, pH 8·2 solution, but gave nevertheless smaller humps. Secondly, BAPTA solutions blocked Ca-dependent humps more efficiently than EGTA solutions of equal equilibrium buffering capacity.

Ca currents in Cs-dialysed cells

Some of the differences in K currents observed among the solutions listed in Table 1 might have been due to changes in Ca currents. This possibility was examined in a series of experiments where Ca currents were measured in cells dialysed with a solution containing Cs instead of K, and including 20 mM-tetraethylammonium (TEA). The results are included in Table 2. It appears that Ca-current amplitude is not significantly affected by changing the EGTA concentration from 0·5 to 10 mM, or by increasing the pH from 7·2 to 8·2. In the 11 mM-EGTA/1 mM-Ca, pH 8·2

solution, the $I-V$ curve was displaced by about 10 mV to the right along the voltage axis. This shift may have been a consequence of a change of the surface potential at the cytoplasmic side of the membrane as the free-Mg concentration was reduced.

The Ca-current amplitudes of Fig. 2 are very similar to those found previously with the 11 mM-EGTA/1 mM-Ca, Cs-rich solution (Fenwick *et al.* 1982*b*). They are also close to those found previously in Na-dialysed cells (Clapham & Neher, 1984). Finally, estimates obtained from noise analysis to be presented below, again gave very similar values in K-dialysed cells. Thus, the peak value of Ca currents does not vary strongly with the nature of the internal cation.

Effects of internal Mg ions

Due to the finite affinity of EGTA to Mg, it was impossible to maintain the free-Mg concentration of all internal solutions at the standard value of 2 mM (see Table 1). As mentioned in the preceding section (and in an earlier study, Fenwick *et al.* 1982*b*), 2 mM-Mg does not affect Ca currents much apart from a 10 mV shift. It seemed, however, possible that internal Mg ions could change the properties of one or several of the K channels described below. This has been shown for BK channels, the opening probability of which is increased by internal Mg at low Ca concentrations (A. Marty, unpublished results). But in control experiments, very similar Ca-dependent humps were obtained in 11 mM-EGTA/1 mM-Ca solutions whether or not 2 mM-Mg was added. The major difference found between the two situations was a small displacement of $I-V$ curves towards more positive potentials with the Mg-free solution, which matched the shift of Ca currents mentioned above.

A curious additional difference was noted. In Mg-free solutions, Ca-dependent currents inactivated at those potentials where they were largest. This effect developed only after a few minutes of whole-cell recording. It was also observed with the solutions of Table 1 which had a low free-Mg concentration. It is possible that Ca currents inactivate more in Mg-free solutions than in control conditions. Similarly, we observed that Ca-dependent currents had a tendency to inactivate with the 0·5 mM-EGTA solution, and we also attributed this to inactivation of the underlying Ca currents. Further work would be needed to ascertain whether Ca-current decline is indeed affected by internal Mg and by EGTA concentration.

Noise analysis of Ca-independent K currents

In 'ensemble noise' analysis, individual current traces, which contain fluctuations due to variations of the number of open channels, are compared to the average of many traces, where the fluctuations are smoothed out (Sigworth, 1980). Fig. 5*A* displays single sweep and averaged records obtained at 10 mV in normal saline after complete run-down of Ca currents. Analysis of the single sweep fluctuations yields the mean variance shown in Fig. 5*B*. When plotted against mean current, the mean variance may be approximated by a model parabolic curve giving an apparent elementary current value, I_{el}, of 1·5 pA, a total number of channels, N, of 620, and a maximal channel opening probability, P_o, of 0·60. Six experiments gave I_{el} values ranging between 0·85 and 1·5 pA, and N values between 150 and 1700. Average values from these experiments are shown in Table 3. These figures must be taken with great caution, however, because one of the main assumptions underlying the analysis,

according to which the outward current is due to a single class of channels, is not supported by additional results. First, outside-out patches studied under the same ionic conditions as those of Fig. 5 had two, not one, channel types likely to contribute to the mean current and mean variance of the macroscopic current. Secondly, when mean current *versus* mean variance plots were made for a given cell at various potentials and parabolas fitted to the results, the value of N obtained from the fits varied greatly with voltage. In the experiments of Fig. 5, for instance, fitted N values

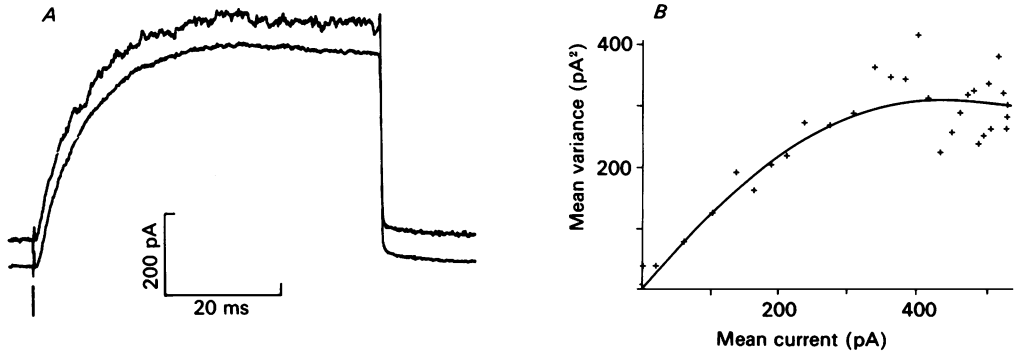

Fig. 5. Noise analysis of K currents after run-down of Ca currents. *A*, single sweep and mean current responses to 90 mV voltage steps from −80 mV. Records obtained in normal saline after complete run-down of Ca currents. *B*, mean variance *versus* mean current analysis of the results in *A*, carried out on thirty-two sweeps. A parabola has been fitted by eye to the data points, yielding $I_{el} = 1{\cdot}4$ pA, $N = 620$ and $P_o = 0{\cdot}60$.

increased continuously from −30 mV (where the fit gave $I_{el} = 0{\cdot}70$ pA and $N = 283$) to +20 mV (with $I_{el} = 1{\cdot}3$ pA and N estimated above 1000).

In the experiment of Fig. 5 fluctuations of K currents could be studied independently of Ca entry because no functional Ca channels remained in the membrane. Identical results were obtained with and without external Ca ions. The other approach was to study the noise of outward currents in Ca-free solution before run-down. A difficulty arose then due to the presence of monovalent ion currents through Ca channels. These currents are, however, close to their reversal between −10 and +10 mV, so that the error was probably small in this potential range. Results obtained at +10 mV before and after run-down gave indeed similar I_{el} and N values. The two experimental situations have therefore not been distinguished in the average values given in Table 3; the corresponding currents have been termed 'background current' in this Table to contrast them with the Ca-dependent K current.

Fluctuations of Ca-dependent K currents

Fig. 6*A* compares traces obtained in the presence and in the absence of external Ca. The test potential was +10 mV, where the Ca-dependent hump is maximal. Comparison between single sweep and averaged traces reveals larger and slower fluctuations in the presence of Ca than in its absence. To analyse the Ca-dependent fluctuations further, both mean variance and mean current obtained in Ca-free

solution were subtracted from the corresponding results in 1 mM-Ca (Fig. 6*B*). The resulting mean current displays an inward transient of 70 pA, corresponding to the early activation of the Ca current. The presence of this inward Ca current must be taken into account when interpreting the mean variance *versus* mean current plot, shown in Fig. 6*C*. Because Ca currents have a very low unit size in 1 mM-external Ca

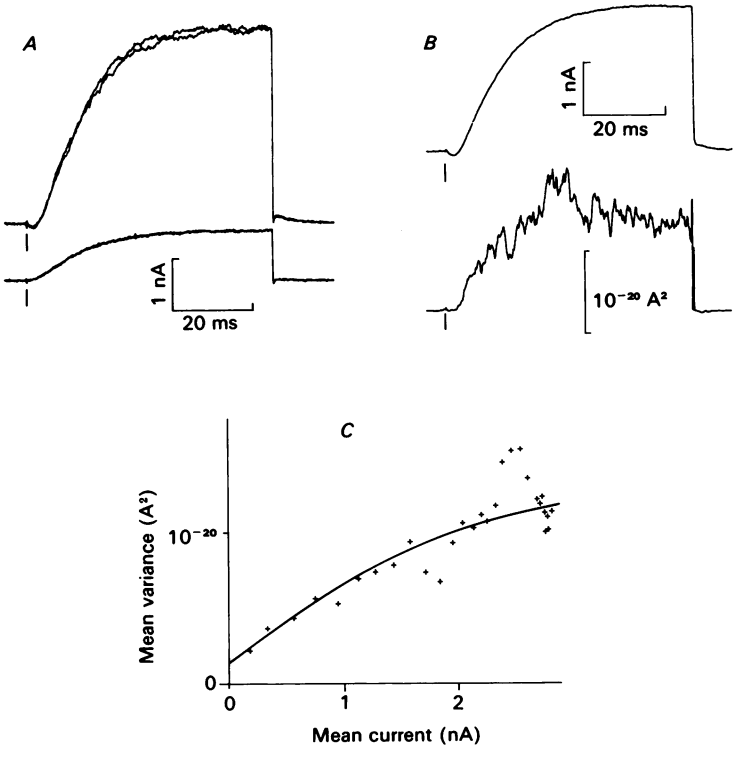

Fig. 6. Noise analysis of Ca-dependent current. Test potential +10 mV, as in Fig. 5. *A*, pairs of responses to voltage steps in normal saline (above) and in Ca-free saline (below). Leakage and capacitive currents have been subtracted. The two traces in Ca-free saline are hardly distinguishable. However, the currents in normal solution show marked differences between consecutive pulses. *B*, mean (above) and mean variance (below) of the Ca-dependent current shown in *A*. Both curves represent differences between values in normal saline and Ca-free saline. *C*, plot of the results in *B*. The points start 4·5 ms after the beginning of the voltage steps. Parameters of the model parabola: I_{el} = 6·5 pA; N = 1000; P_o = 0·40; offset current −180 pA (due to Ca current).

(about 0·02 pA: Fenwick *et al.* 1982*b*), their contribution to the total variance can be neglected. Also, the Ca current has a comparatively fast turn on, activating completely within 5 ms after a voltage step to +10 mV in low Ca solutions (Fenwick *et al.* 1982*b*). We therefore assumed the Ca current to be constant during the test pulse, so that its presence would result in a simple displacement of the variance current relationship along the current axis. When allowing this shift to be an additional free parameter in the fitting procedure, the Ca current (which cannot be measured directly in a K-dialysed cell) was estimated to be 26±23 pA/pF (mean±S.D.), which

compares to 21 ± 13 pA/pF (mean $\pm$ S.D.) in Cs-dialysed cells (Table 2). Taking this shift into account the mean variance plot could be fitted by a parabola (Fig. 6*C*).

Values of the unitary current derived from such fits were 4- to 8-fold larger than those obtained in Ca-free solution. Averaged results from six experiments similar to that of Fig. 6 are presented in Table 3. At +10 mV, the mean elementary current value was 6·8 pA, a value very close to that (6·5 pA) measured directly on the class

TABLE 3. Noise characteristics of background K current and of Ca-dependent K current at +10 mV

	I_{el} (pA)	P_o	N	Number of cells
Background current	$1{\cdot}08 \pm 0{\cdot}22$	$0{\cdot}55 \pm 0{\cdot}10$	835 ± 500	6
Ca-dependent current	$6{\cdot}8 \pm 0{\cdot}74$	$0{\cdot}54 \pm 0{\cdot}14$	541 ± 263	6

Means $\pm$ standard deviations. A total of eight experiments were analysed; four gave usable results at +10 mV both for the background and for the Ca-dependent current.

of Ca-dependent K channels described earlier in isolated patches (Marty, 1981). We shall call these channels BK channels hereafter.

The results of Table 3 give strong evidence in favour of a role of BK channels in the generation of the Ca-dependent hump. Particularly, the close agreement between the noise estimate of the Ca-dependent component and the unit amplitude of the BK channels rules out any significant contribution of small conductance channels (like those observed by Lux, Neher & Marty, 1981) to the Ca-dependent current.

In one experiment, where ensemble fluctuation analysis was carried out at 0, +10 and +20 mV, I_{el} values close to those measured for BK channels were obtained at all potential values. Interestingly, identical N values could be chosen at all potentials. Likewise, results obtained at a given potential during run-down could be fitted with constant N and I_{el} values, simply by decreasing the maximum fraction of open channels. This shows that run-down here is not due to a change in the number of functional BK channels but to a declining supply of Ca. Noise results on Ca-dependent currents did not show the anomalous variations of N found with the currents measured in Ca-free saline. On this basis alone, the currents are more likely to be due to a single population of channels in the former case than in the latter.

Cell-attached experiments

Ca-dependent activation of BK channels was directly observed in cell-attached experiments by depolarizing the membrane either by a voltage step or by changing rapidly the external solution with an isotonic KCl solution containing 1 mM-Ca. The latter solution was applied for about 200 ms with the fast microperfusion system. During application, the cell was depolarized entirely, and BK channels were activated. On the other hand, depolarizing the patch to 0 mV failed to elicit BK channel activity. (The pipette solution did not contain Ca, so that the depolarizing pulses did not provoke Ca entry by themselves.) These experiments showed that BK channels were selectively activated by Ca entry under conditions where the cells kept their normal intracellular medium. Previous cell-attached experiments had already shown BK-channel activation during action potentials (Fenwick *et al.* 1982*a*).

Effects of TEA and quinine

TEA and quinine (or its stereoisomer quinidine) have been shown to block the Ca-induced hump of K currents in several preparations: for review of TEA effects see Stanfield (1983); Hermann & Gorman (1984). In chromaffin cells, both drugs reversibly block single-channel currents through BK channels (A. Marty, unpublished observations). Fig. 7 shows the results of two experiments where 1 mM-TEA and

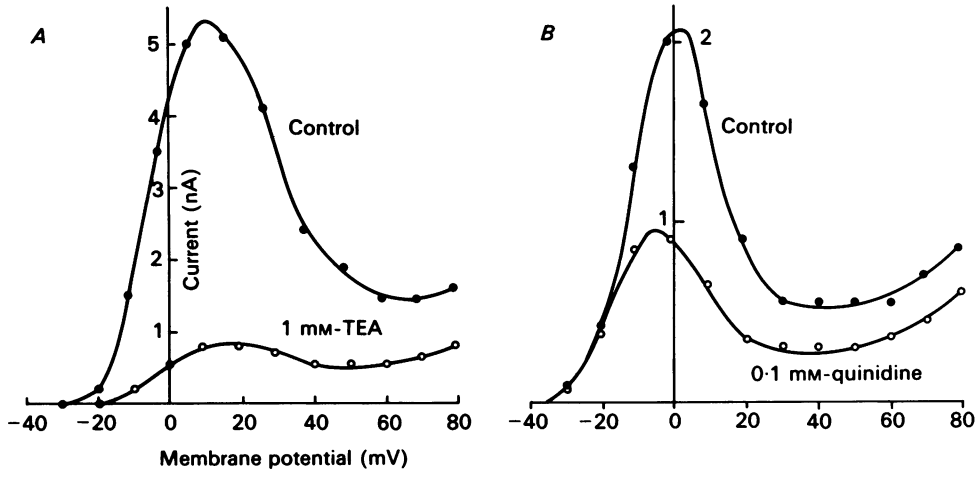

Fig. 7. Reduction of outward currents by 1 mM-tetraethylammonium (*A*) and by 0·1 mM-quinidine (*B*). Peak outward current is plotted as a function of test potential with standard external saline (control) and the indicated drug concentration added. Conditions are similar to those of Fig. 1, except that the internal solution contained approximately 10 mM-Na ions.

0·1 mM-quinidine reduced the Ca-dependent K currents (measured by the graphic method of Fig. 3) to 13% (Fig. 7*A*) and to 44% (Fig. 7*B*) of their initial size, respectively. These observations are consistent with the hypothesis that BK channels underlie the Ca-dependent hump. However, neither TEA nor quinidine can be considered as a selective blocker of this current at the concentrations used, since in outside-out patches both drugs were found to inhibit significantly the single-channel activity associated not only with BK channels, but also with the smaller conductance channels to be described below.

Three types of single-channel outward currents

The noise analysis above indicated that in the presence of external Ca, BK channels contribute the major part of outward current around 0 mV. In the absence of Ca, noise analysis indicated much smaller unit current events. However, the data were not compatible with a homogeneous population of channels under these conditions.

Single-channel recordings performed on outside-out patches confirmed these conclusions. In a typical patch with standard salines inside and outside (TTX added to the outside) three types of channels could be observed which are well separated

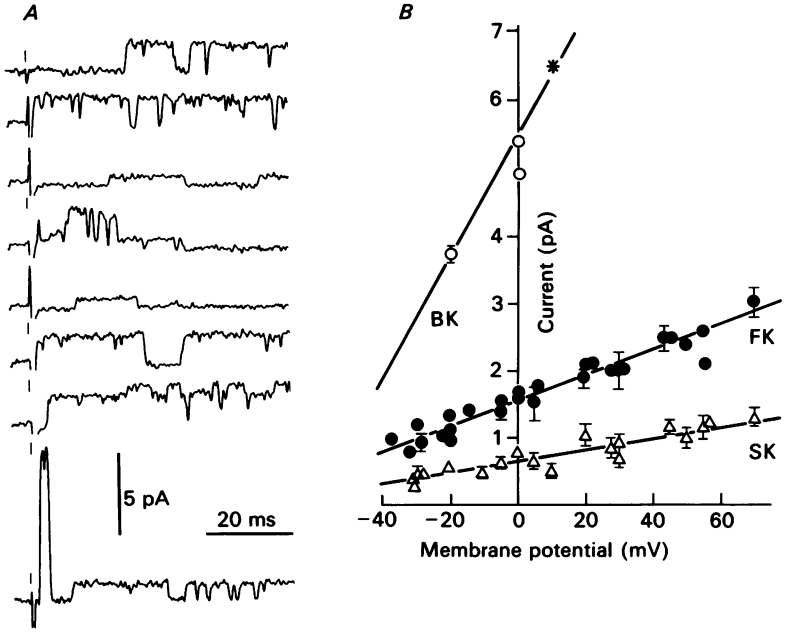

Fig. 8. Single-channel amplitudes. Three types of outward currents can be distinguished by amplitudes. *A* shows representative examples from outside-out patches with a mixed population of channels. The upper seven traces are from a patch the potential of which was stepped to 0 mV. FK and SK channels alternate or superimpose in consecutive traces. The last trace is from another patch which was jumped to 20 mV. Here one BK and one SK channel is active. Current records in this and the subsequent Figures were digitized as described in Methods and were plotted on an electrostatic plotter after splining (see Sigworth, 1983*a*). Standard external and internal solutions (the latter containing 11 mM-EGTA/1 mM-Ca) were used: holding potential −80 mV, 25–28 °C. *B* gives pooled amplitude data from five outside-out patches at 21–24 °C. Error bars, where given, represent standard deviation within readings from one patch. The asterisk is a value taken from Marty (1981). The lines are linear regressions with the following values: SK: x intercept −82 mV; slope 8·4 pS. FK: x intercept −84 mV, slope 18·4 pS. BK: x intercept −60 mV, slope 96 pS (most of the BK data points lie outside the range of this Figure). In another series of experiments performed on a warm summer day (25–28 °C) the slope conductances were 12 pS for SK channels and 20 pS for FK channels.

by amplitude (Fig. 8*A*). A plot of the three classes of single channel amplitudes *versus* voltage (Fig. 8*B*) yielded slope conductance values of 8 pS, 18 pS and 96 pS. Under our recording conditions (11 mM-EGTA inside) the large (96 pS) channel appeared only rarely in the voltage range −20 to +30 mV. However, it was abundant at high positive potentials. This channel is the Ca-activated BK channel described previously (Marty, 1981). It will not be considered further here. The two small-type channels are voltage dependent and will be termed SK (small amplitude or slow K channel, 8 pS) and FK (fast K channel, 18 pS), respectively. It was observed that the amplitudes of the SK channels scattered more than was expected from the background noise. They also scattered more than the values of the FK channels.

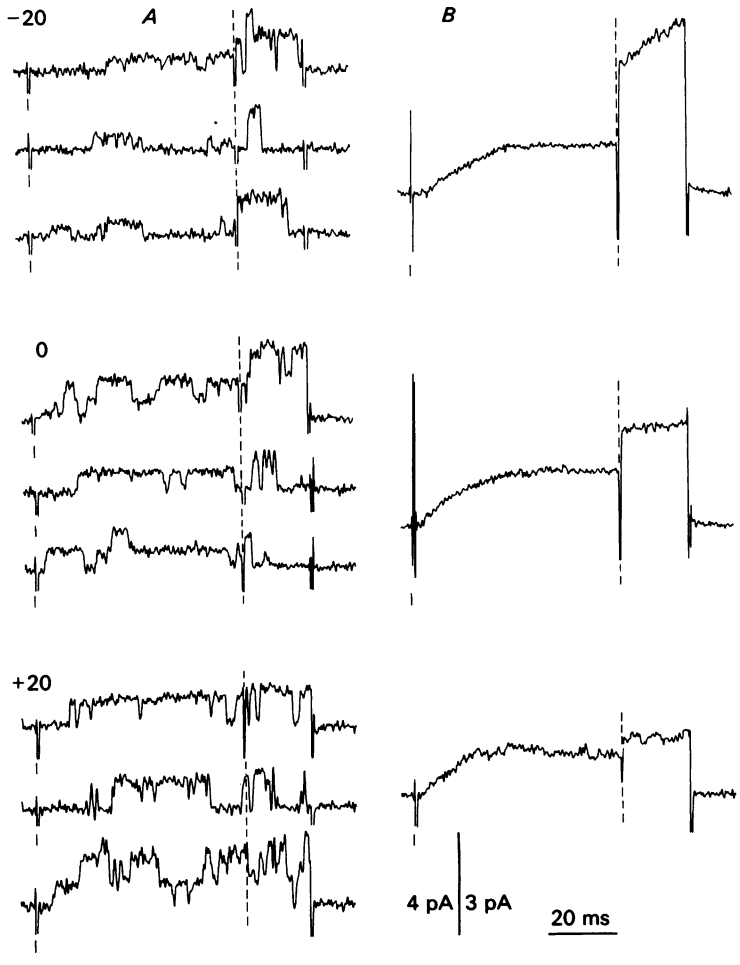

Fig. 9. A patch which contained only SK and BK channels. The outside-out patch was held at −80 mV. First, the potential was stepped to the indicated value (−20, 0 or +20 mV) and at the time of the dashed line the potential was stepped to +40 mV. *A* gives individual traces, *B* gives averages of 30–100 traces each. There is a pronounced decrease in channel opening frequency during the whole experiment, such that averaged currents are very small in the last run (at +20 mV). For −20 mV and 0 mV averages all records were included which did not contain BK-channel openings, including blank records. For the +20 mV average, episodes of higher activity (excluding blanks) were selected in order to obtain better signal to noise ratio. Recording conditions are the same as those of Fig. 8*A*.

Kinetic differences between SK and FK channels

Occasionally patches were obtained which contained only one type of channel in addition to BK channels. These patches were selected for analysis in order to study the properties of SK and FK channels individually. We wanted to obtain average time courses of activation and inactivation at given voltages, as well as steady-state opening probabilities as a function of voltage. The latter measurement presented

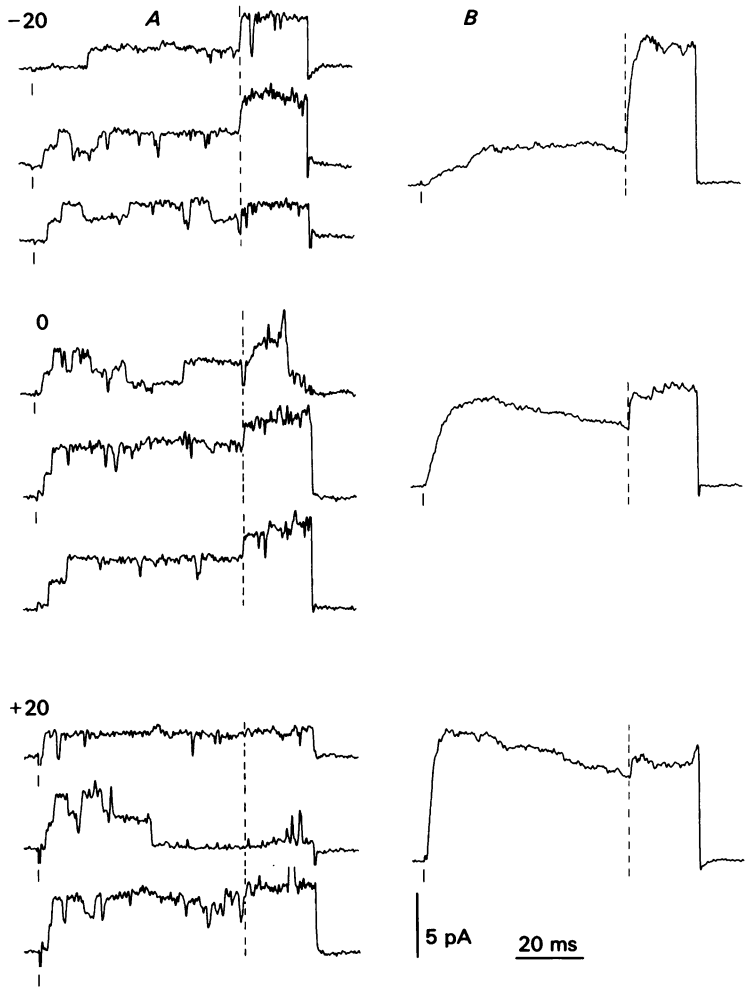

Fig. 10. A patch which contained only FK and BK channels. Records in analogy to those of Fig. 9. The lowermost trace at +20 mV contains a BK-channel opening which is truncated.

some difficulty, since it appeared that the number of active channels fluctuated between sweeps. These fluctuations probably reflect a process of slow inactivation. We therefore adopted a two-pulse protocol to compare the mean number of open channels ($\bar{n}$) at some test voltage (V), $\bar{n}$ (V), with the same quantity $\bar{n}$ (V_{ref}) at a reference potential, V_{ref}. For this, the patch potential was stepped from a holding value of −80 to a test potential of either −20 mV, 0 mV or +20 mV for 60 ms and then stepped to +40 mV for a further 20 ms. The reference potential of +40 mV was chosen because at higher values interference from BK channels would have been prohibitively large.

Fig. 9*A* shows individual records from a patch which had exclusively SK channels (apart from occasional BK-channel openings). Fig. 9*B* shows ensemble averages of

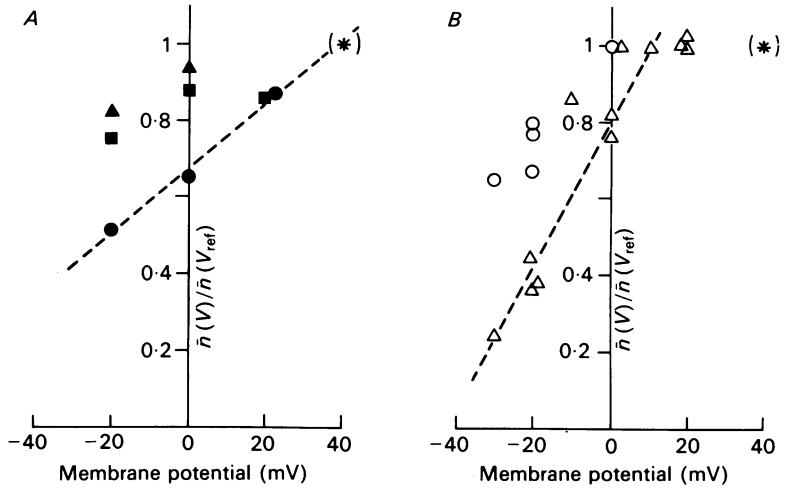

Fig. 11. Voltage dependence of relative opening probability. Records like those of Figs. 9*B* and 10*B* were analysed to determine the ratio between mean number of open channels $\bar{n}(V)$ at the end of the test episode at potential V and mean number of open channels $\bar{n}(V_{ref})$ at the reference potential V_{ref}. V_{ref} was +40 mV except for four data points in *B* where the whole pulse sequence was shifted by 10 mV ($V_{hold} = -90$ instead of -80; $V_{ref} = 30$ instead of 40). In *A* two recordings were analysed which contained exclusively SK channels (●, ■); one patch contained both SK and FK channels (▲). In the latter case averages were taken from only those traces which did not contain any FK-channel opening. In *B* five patches (pooled into two groups, see below) were analysed which contained at least one more FK channel than SK channel. Under these conditions the average behaviour is determined by the FK channel. The quantity plotted is the ratio between current values at the ends of the two episodes divided by the ratio of single-channel currents at the corresponding voltages (see text). In cases where inactivation was evident during the episode at V_{ref} the mean current value was back extrapolated (disregarding a fast activation phase) to the onset of the V_{ref} episode. The ratio of single-channel amplitudes was determined individually for each run in order to eliminate scatter due to the non-homogeneity in SK single-channel amplitudes (except for one patch in *B* where average values were taken). The data show large scatter, mainly due to a shift in channel parameters along the voltage axis following patch isolation (Marty & Neher, 1983; Fernandez, Fox & Krasne, 1984). Therefore the data points of *B* were separated into two groups according to whether they were taken early (△) or late (○) after establishment of the outside patch configuration. Early means that the data come from the first series of pulses which was usually completed within three to five minutes after patch formation. A line is drawn in *B* connecting early points to indicate the steepness of the relation. Another line is drawn in *A* connecting data points of a particular patch. The values at +40 mV are given in brackets since they are 1 by definition.

all those traces which did not contain BK-channel openings. Note the relatively slow time course of activation and the absence of inactivation at this time scale. SK channels did inactivate, however, if the patch was held at depolarized potentials (−20 mV to +20 mV) for prolonged periods. Under these conditions both SK and FK channels disappeared completely. The only unit activity that remained, consisted of occasional BK channels and some very small conductance channels (<5 pS) that were not investigated further. Fig. 10 shows the same kind of results as Fig. 9, obtained on a patch which contained FK channels instead of SK channels.

SK and FK channels have different voltage dependence

In order to assess the voltage dependence of the opening probability we formed ratios between the mean current at the end of the test period $\bar{I}(V)$ and that at the end of the reference episode $\bar{I}(V_{ref})$ at 40 mV. This ratio was divided by the ratio of single-channel amplitudes at the two voltages, obtained from the same set of records.

This quantity is the ratio between the mean numbers of open channels at the two potentials under steady state and is plotted in Fig. 11*A versus* voltage. It approaches the ratio of opening probabilities as the number of records becomes large, provided that the number of participating channels in any one record is constant. Fig. 11*A* shows that the voltage dependence of the SK channels is not very steep. Unfortunately, the scatter is rather large, possibly due to slow shifts along the voltage axis of voltage-dependent parameters following patch isolation (Marty & Neher, 1983; Fernandez *et al.* 1984). In the patch that yielded the most extensive data (circles in Fig. 11*A*), it was clear that the open probability continued to increase with potential up to and probably beyond 40 mV indicating that saturation occurs only at potentials larger than 40 mV.

Contrary to these results, an analogous analysis on patches which predominantly contain FK (18 pS) channels, shows a steeper voltage dependence which saturates between +20 and +40 mV (see Fig. 11*B*). The activation kinetics of these channels were much faster (Fig. 10*B*) and most patches displayed clear inactivation in a 60 ms period at 0 and +20 mV. Inspection of single-channel records shows that those channels which do not inactivate during the 60 ms test period are almost permanently open at +40 mV, apart from short closing flickers. From this we conclude that, disregarding the slow inactivation process, the opening probability of FK channels is close to 1 at +40 mV.

For the SK channel a different conclusion is suggested from the voltage dependence displayed in Fig. 11*A* as discussed above. We tried to estimate the opening probability at +40 mV, again disregarding inactivation. Inactivation is slow compared to a sweep duration, as indicated by the average time course. From that it follows that the number of active channels does not very often change during one record. At +20 mV we could often observe sequences of sweeps which had openings but no overlaps of channels. It is then very likely that in these sweeps only one channel was operative (not inactivated). This is so because under these conditions, both mean channel open times and mean channel close times are around 5–10 ms values which assure that the probability of observing at least one opening during a 80 ms sweep is high if a channel is active, and that overlaps are seen if more than one channel is active. We took averages of those sweeps which had at least one opening but no overlaps and divided the mean current at the end of the +40 mV segment by the single-channel amplitude. This resulted in estimates of the opening probability at +40 mV between 0·38 and 0·5. A similar analysis on an ensemble of FK records (test potential 0 mV; reference potential +40 mV) gave an opening probability at +40 mV of 0·6. However, this low value is almost entirely due to inactivation since the average current had decreased during the preceding test period by 32 % (measured from its peak).

Relation between single-channel and whole-cell currents

In our experiments the majority of patches had mixed populations of channels. We did not perform statistics of their relative appearance, since in many patches the number of channels was not stationary but decreased during prolonged runs lasting 10 min or more. (Actually we never knew the total number of channels present due to the problem of inactivation addressed above.) Channels in mixed patches clearly belonged to one of the two types characterized above since selected sweeps which

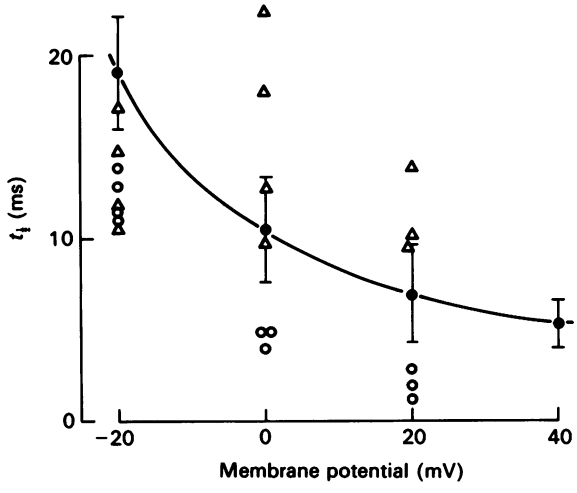

Fig. 12. Comparison of the rise times of whole-cell currents with values for the two types of channels. The time to half-maximum outward current ($t_{\frac{1}{2}}$) is plotted *versus* membrane potential. Mean values ± standard deviations are given for six (values between −20 and +20 mV) or three (at +40 mV) recordings (●). They are connected by a line drawn by eye. Only those whole-cell recordings were evaluated for the Figure where Ca-dependent currents had essentially vanished. In addition, values of average currents from outside-out patches containing only FK channels (○) and values from patches containing only SK channels (△) are given. FK values are exclusively early estimates (see legend to Fig. 11) whereas SK values are mostly late estimates.

contained only one type gave ensemble averages very similar to one of the two examples shown in Figs. 9 and 10.

We tried to estimate the relative contributions of the two types to the Ca-independent whole-cell current by comparing rise times of whole-cell currents with those of the two types under conditions where Ca-dependent current is not present. Fig. 12 plots $t_{\frac{1}{2}}$ (the time to half-maximum current) values for the rising phase of whole-cell currents and of ensemble-averaged currents from patches with the one or the other type channel. It is seen that whole-cell values lie in between these two extremes with some scatter. Probably individual cells possess varying proportions of SK and FK channels. However, a sizeable fraction of total Ca-independent current must be carried by SK channels since basically all cells show some slowly rising net current when stepping the potential to +20 or +40 mV. Obviously, slow activation of SK

current supersedes inactivation which would be expected to result from the kinetics of FK channels.

The conclusion that both SK and FK channels contribute significantly to the whole-cell current is corroborated by the results of Table 3, which gives at +10 mV an apparent elementary current value lying midway between unitary currents of SK and FK channels (Fig. 8).

DISCUSSION

The K channels observed in bovine chromaffin cells fall into three classes. With low internal Ca concentration, and no Ca outside, mostly two relatively small conductance-channel types (FK and SK channels) contribute to the cell current up to about +40 mV. The unit conductance of one of these (FK) is approximately twice that of the other one. Both types of channels display burst kinetics, and both inactivate. However, activation and inactivation rates are much faster for FK than for SK channels. Another difference between the two types of channels arises from the shape of the conductance–voltage curves, which is steeper for the FK channel. Both channels give rise to much smaller single currents than the third type (BK channel) which is Ca activated.

Two components of the cell outward current are linked to Ca channels. First, above +50 mV, there is a surprisingly large outward current component carried by K ions crossing Ca channels. Secondly, a Ca-dependent component peaking around +10 mV is observed in the presence of extracellular Ca. The two types of currents gradually decline during run-down of Ca channels. BK channels not only underlie the Ca-dependent hump peaking at +10 mV, but also constitute a sizeable part of the current above +30 mV.

BK, FK and SK channels, together with Ca channels, appear to account almost entirely for the outward currents of chromaffin cells. It is of course difficult to rigorously rule out the presence of yet another component and indeed outside-out patch experiments do indicate the presence of an additional channel with very low unitary conductance. However, this channel probably accounts for only a very modest part of the total current.

Our finding that the Ca-dependent hump of chromaffin cell currents is due to the large unitary conductance BK channels contrasts with a noise analysis of a similar current in snail neurones giving a 15–18 pS unitary conductance (Hermann & Hartung, 1982). This lower value corresponds to the unit conductance of the Ca-dependent channels observed in certain snail neurones (Lux, Neher & Marty, 1981). Thus, two currents which macroscopically look almost identical turn out to be carried by very distinct classes of channels. Our finding that the noise estimate for the Ca-dependent current agrees closely with the single-channel BK value rules out any major participation of a smaller conductance Ca-activated channel. This is different from the case of bull-frog ganglion cells where two different Ca-dependent K channels are postulated (Pennefather, Lancaster, Adams & Nicoll, 1985). Our finding of two Ca-independent K channels, on the other hand, is not surprising in view of kinetic studies (Dubois, 1983) and noise analyses (Conti, Hille & Nonner, 1984) on delayed rectifier currents in frog node.

FK channels of chromaffin cells resemble closely the channels recently described by Ypey & Clapham (1984) in macrophages. Also, channels similar to SK and FK channels are present in lymphocytes (Cahalan, Chandy, DeCoursey & Gupta, 1985).

Knowing from the results of noise analysis (Table 3) the probability of BK channels to be open, P_o, when the membrane potential is stepped to +10 mV in the presence of external Ca, it is possible to obtain a rough estimate of the Ca concentration attained in the vicinity of the membrane. Inside-out experiments show that such P_o values are obtained between 0·5 and 1 μM-internal Ca at membrane potentials of 0 or +20 mV (A. Marty, unpublished results). At higher internal Ca levels, P_o becomes largely independent of voltage and of internal Ca. In the present experiments, we saw no sign of saturation near the peak of Ca-dependent currents. Thus, the effective value of internal Ca concentration was probably close to 1 μM.

Such a high internal Ca value is surprising in a cell dialysed with comparatively large concentrations of EGTA or BAPTA. The possibility that such a high internal Ca value would be homogeneous over the entire cell volume can be easily dismissed. Apparent rates of Ca binding by EGTA are $>10^6$/M.s at pH 7·2 (Smith, Berger & Podolsky, 1977). Thus, a typical influx of approximately 5×10^{-4} M/s would produce a steady-state internal Ca elevation smaller than 0·05 μM at 10 mM of free EGTA, if Ca would equilibrate rapidly by diffusion throughout the cell volume. It has to be postulated therefore that the increase in internal Ca is restricted to the very vicinity of the membrane.

Calculations concerning Ca buffering and Ca diffusion in the vicinity of a membrane have been performed for fixed Ca-uptake sites (Fischmeister & Horackova, 1983; Zucker & Stockbridge, 1983; Chad & Eckert, 1984). However, to our knowledge the diffusion profile of Ca in the presence of high concentrations of diffusible buffer has not been determined. Therefore, at present we cannot comment on the physical basis of the internal Ca gradient.

We thank Mr M. Pilot for optimizing the cell preparation technique. A.M. was supported by C.N.R.S. and I.N.S.E.R.M. (contract no. 836023). E.N. was supported by a grant from the Deutsche Forschungsgemeinschaft (DFG).

REFERENCES

ALMERS, W. & MCCLESKEY, E. W. (1984). Non-selective conductance in calcium channels of frog muscle: calcium selectivity in a single-file pore. *Journal of Physiology* **353**, 585–608.

ALMERS, W., MCCLESKEY, E. W. & PALADE, P. T. (1984). A non-selective cation conductance in frog muscle membrane blocked by micromolar external calcium ions. *Journal of Physiology* **353**, 565–583.

BIALES, B., DICHTER, M. & TISCHLER, A. (1976). Electrical excitability of cultured adrenal chromaffin cells. *Journal of Physiology* **262**, 743–753.

BRANDT, B. L., HAGIWARA, S., KIDOKORO, Y. & MIYAZAKI, S. (1976). Action potentials in the rat chromaffin cell and effects of acetylcholine. *Journal of Physiology* **263**, 417–439.

CAHALAN, M. D., CHANDY, K. D., DECOURSEY, T. E. & GUPTA, S. (1985). A voltage-gated potassium ion channel in human T lymphocytes. *Journal of Physiology* **358**, 197–237.

CHAD, J. E. & ECKERT, R. (1984). Calcium domains associated with individual channels can account for anomalous voltage relations of Ca-dependent responses. *Biophysical Journal* **45**, 993–999.

CLAPHAM, D. E. & NEHER, E. (1984). Trifluoperazine reduces inward ionic currents and secretion by separate mechanisms in bovine chromaffin cells. *Journal of Physiology* **353**, 541–564.

CONTI, F., HILLE, B. & NONNER, W. (1984). Non-stationary fluctuations of the potassium conductance at the node of Ranvier of the frog. *Journal of Physiology* **353**, 199–230.

DUBOIS, J. M. (1983). Potassium currents in the frog node of Ranvier. *Progress in Biophysics and Molecular Biology* **42**, 1–20.

FENWICK, E. M., MARTY, A. & NEHER, E. (1982*a*). A patch-clamp study of bovine chromaffin cells and of their sensitivity to acetylcholine. *Journal of Physiology* **331**, 577–597.

FENWICK, E. M., MARTY, A. & NEHER, E. (1982*b*). Sodium and calcium channels in bovine chromaffin cells. *Journal of Physiology* **331**, 599–635.

FERNANDEZ, J. M., FOX, A. P. & KRASNE, S. (1984). Membrane patches and whole-cell membranes: a comparison of electrical properties in rat clonal pituitary (GH_3) cells. *Journal of Physiology* **356**, 565–585.

FISCHMEISTER, R. & HORACKOVA, M. (1983). Variation of intracellular Ca^{2+} following Ca^{2+} current in heart. A theoretical study of ionic diffusion inside a cylindrical cell. *Biophysical Journal* **41**, 341–348.

HAMILL, O. P., MARTY, A., NEHER, E., SAKMANN, B. & SIGWORTH, F. J. (1981). Improved patch-clamp techniques for high-solution current recording from cells and cell-free membrane patches. *Pflügers Archiv* **391**, 85–100.

HERMANN, A. & GORMAN, A. L. F. (1984). Action of quinidine on ionic currents of molluscan pacemaker neurons. *Journal of General Physiology* **83**, 919–940.

HERMANN, A. & HARTUNG, K. (1982). Noise and relaxation measurements of the Ca^{2+} activated K^+ current in helix neurones. *Pflügers Archiv* **393**, 254–261.

HERMANN, A. & HARTUNG, K. (1983). Ca^{2+} activated K^+ conductance in molluscan neurones. *Cell Calcium* **4**, 387–405.

HESS, P. & TSIEN, R. W. (1984). Mechanisms of ion permeation through calcium channels. *Nature* **309**, 453–456.

HEYER, C. B. & LUX, H. D. (1976). Control of the delayed outward potassium currents in bursting pace-maker neurones of the snail, *Helix pomatia*. *Journal of Physiology* **262**, 349–382.

KIDOKORO, Y. & RITCHIE, A. K. (1980). Chromaffin cell action potentials and their possible role in adrenaline secretion from rat adrenal medulla. *Journal of Physiology* **307**, 199–216.

KOSTYUK, P. G. & KRISHTAL, O. A. (1977). Effects of calcium and calcium-chelating agents on the inward and outward currents in the membrane of mollusc neurones. *Journal of Physiology* **270**, 569–580.

KOSTYUK, P. G., MIRONOV, L. S. & SHUBA, YA. M. (1983). Two ion-selecting filters in the calcium channel of the somatic membrane of mollusc neurons. *Journal of Membrane Biology* **76**, 83–93.

LEE, K. S. & TSIEN, R. W. (1982). Reversal of current through calcium channels in dialysed single heart cells. *Nature* **297**, 498–501.

LUX, H. D., NEHER, E. & MARTY, A. (1981). Single channel activity associated with the calcium dependent outward current in *Helix pomatia*. *Pflügers Archiv* **389**, 293–295.

MARTELL, A. E. & SMITH, R. M. (1974). *Critical Stability Constants. Amino Acids*, vol. 1, New York: Plenum Press.

MARTY, A. (1981). Ca-dependent K channels with large unitary conductance in chromaffin cell membrane. *Nature* **291**, 497–500.

MARTY, A. & NEHER, E. (1983). Tight-seal whole-cell recording. In *Single Channel Recording*, ed. SAKMANN, B. & NEHER, E., pp. 107–122. New York and London: Plenum Press.

MEECH, R. W. & STANDEN, N. B. (1975). Potassium activation in *Helix aspersa* neurones under voltage clamp: a component mediated by calcium influx. *Journal of Physiology* **249**, 211–239.

PENNEFATHER, P., LANCASTER, B., ADAMS, P. R. & NICOLL, R. A. (1985). Two distinct Ca-dependent K currents in bullfrog sympathetic ganglion cells. *Proceedings of the National Academy of Sciences of the U.S.A.* **82**, 3040–3044.

SIGWORTH, F. J. (1980). The variance of sodium current fluctuations at the node of Ranvier. *Journal of Physiology* **307**, 97–129.

SIGWORTH, F. J. (1983*a*). An example of analysis. In *Single Channel Recording*, ed. SAKMANN, B. & NEHER, E., pp. 301–321. New York and London: Plenum Press.

SIGWORTH, F. J. (1983*b*). Electronic design of the patch clamp. In *Single Channel Recording*, ed. SAKMANN, B. & NEHER, E., pp. 3–35. New York and London: Plenum Press.

SMITH, P. D., BERGER, R. L. & PODOLSKY, R. J. (1977). Stopped-flow study of the rate of calcium binding by EGTA. *Biophysical Journal* **17**, 159a.

STANFIELD, P. R. (1983). Tetraethylammonium ions and the potassium permeability of excitable cells. *Reviews of Physiology, Biochemistry and Pharmacology* **97**, 1–67.

THOMPSON, S. H. & ALDRICH, R. W. (1980). Membrane potassium channels. In *The Cell Surface and Neuronal Function*, ed. COTMAN, C. W., POSTE, R. & NICOLSON, G. L., pp. 49–85. Amsterdam: Elsevier, North-Holland.

TSIEN, R. Y. (1980). New calcium indicators and buffers with high selectivity against magnesium and protons: design, synthesis, and properties of prototype structures. *Biochemistry* **19**, 2396–2404.

YPEY, D. L. & CLAPHAM, D. E. (1984). Development of a delayed outward-rectifying K^+ conductance in cultured mouse peritoneal macrophages. *Proceedings of the National Academy of Sciences of the U.S.A.* **81**, 3083–3087.

ZUCKER, R. S. & STOCKBRIDGE, N. (1983). Presynaptic calcium diffusion and the time courses of transmitter release and synaptic facilitation at the squid giant synapse. *Journal of Neuroscience* **3**, 1263–1269.